

Thermodynamic limit of the six-vertex model with domain wall boundary conditions

V. Korepin *and* P. Zinn-Justin

*C.N. Yang Institute for Theoretical Physics
State University of New York at Stony Brook
Stony Brook, NY 11794-3840, USA*

We address the question of the dependence of the bulk free energy on boundary conditions for the six vertex model. Here we compare the bulk free energy for periodic and domain wall boundary conditions. Using a determinant representation for the partition function with domain wall boundary conditions, we derive Toda differential equations and solve them asymptotically in order to extract the bulk free energy. We find that it is different and bears no simple relation with the free energy for periodic boundary conditions. The six vertex model with domain wall boundary conditions is closely related to algebraic combinatorics (alternating sign matrices). This implies new results for the weighted counting for large size alternating sign matrices. Finally we comment on the interpretation of our results, in particular in connection with domino tilings (dimers on a square lattice).

1. Introduction

The six vertex model is an important model of classical statistical mechanics in two dimensions. It was solved exactly by E. Lieb [1] and B. Sutherland [2] in 1967 by means of Bethe Ansatz. The bulk free energy was calculated in these papers for periodic boundary conditions (PBC). A detailed classification of the phases of the model can be found for example in the book [3].

Earlier, in 1961 Kasteleyn, while studying dimer arrangements on a quadratic lattice, expressed doubts in independence of the bulk free energy on the boundary conditions [4]. For more on dimer arrangements, see [4], [5] and [6]. Interest in this subject was renewed with recent work on domino tilings (which are equivalent to dimers on a square lattice) of an Aztec diamond [7], [8], demonstrating a strong effect of the boundary on a typical domino configuration. Dimers (or domino tilings) can be considered as a particular case of the six vertex model, and therefore a natural question is to investigate the effect of boundary conditions of the thermodynamic limit of the six vertex model.

Independently of this, new boundary conditions of the six-vertex model, the so-called domain wall boundary conditions (DWBC), were first introduced in 1982 [9] (we shall defined them in detail below). An important recursion relation for the partition function was discovered in this paper. Later these recursion relations helped to find a determinant representation for the partition function of the six vertex model with domain wall boundary conditions [10], [11]. The determinant representation simplifies somewhat in the homogeneous case. In this case the partition function satisfy Toda differential equation [12]. In this paper we use this differential equation in order to calculate the bulk free energy for DWBC.

Let us all mention that there is a one to one correspondence between arrow configurations in the six vertex model with DWBC and Alternating Sign Matrices (ASM) [13]. This mapping was used in order to count the number of ASM. More on ASM can be found in [14] and [15].

The plan of the paper is as follows. In Section 2 we define the six-vertex model with domain wall boundary conditions, and derive the determinant representation for the partition function. In Sect 3 we derive Toda differential equation for the partition function. In Sect 4 we consider the thermodynamic limit; we derive the explicit expression of the bulk free energy in the ferroelectric and disordered phases, and compare it with PBC. Finally, in Sect 6 we conclude with some comments on our results and their connection with other subjects (ASM, domino tilings).

2. Determinant representation of the partition function of the six-vertex model

In this section we shall define the *inhomogeneous* six-vertex model with domain wall boundary conditions, and rewrite its partition function as a determinant. We will then particularize our formula to the homogeneous case.

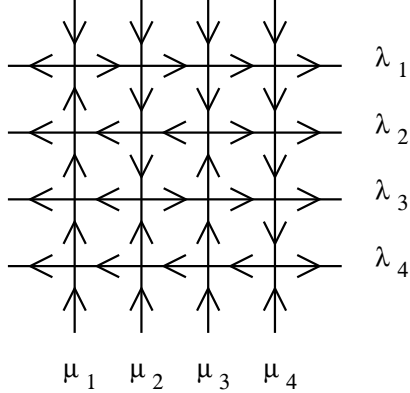


Fig. 1: A configuration of the inhomogeneous six-vertex model with domain wall boundary conditions.

First we define the configurations of the model. They are given by assigning arrows to each edge of a $N \times N$ square lattice (see Fig. 1). The “domain wall” boundary conditions correspond to fixing the horizontal external arrows to be outgoing and the vertical external arrows to be incoming. The partition function is then obtained by summing over all possible configurations:

$$Z = \sum_{\text{arrow configurations}} \prod_{i,k=1}^N w_{ik} \quad (2.1)$$

where the statistical weights w_{ik} are assigned to each *vertex* of the lattice. Since we are considering an inhomogeneous model, we need two sets of spectral parameters $\{\lambda_i\}$ and $\{\mu_k\}$ which are associated with the horizontal and vertical lines. The weight w_{ik} depends on the arrow configuration around the vertex (i, k) and is given by

$$w_{ik} = \begin{cases} a(\lambda_i, \mu_k) & \begin{array}{c} \uparrow \rightarrow \\ \uparrow \leftarrow \\ \rightarrow \end{array} \quad \begin{array}{c} \downarrow \leftarrow \\ \downarrow \rightarrow \\ \leftarrow \end{array} \\ b(\lambda_i, \mu_k) & \begin{array}{c} \uparrow \leftarrow \\ \uparrow \rightarrow \\ \rightarrow \end{array} \quad \begin{array}{c} \downarrow \rightarrow \\ \downarrow \leftarrow \\ \leftarrow \end{array} \\ c(\lambda_i, \mu_k) & \begin{array}{c} \downarrow \rightarrow \\ \downarrow \leftarrow \\ \rightarrow \end{array} \quad \begin{array}{c} \uparrow \leftarrow \\ \uparrow \rightarrow \\ \leftarrow \end{array} \end{cases} \quad (2.2)$$

(all other weights are zero) where the functions a , b , c are chosen as follows:

$$\begin{aligned} a(\lambda, \mu) &= \sinh(\lambda - \mu - \gamma) \\ b(\lambda, \mu) &= \sinh(\lambda - \mu + \gamma) \\ c(\lambda, \mu) &= \sinh(2\gamma) \end{aligned} \tag{2.3}$$

Here γ is an anisotropy parameter which does not depend on the lattice site. The partition function is therefore a function of the $2N$ spectral parameters and we shall denote it by $Z_N(\{\lambda_i\}, \{\mu_k\})$.

The model thus defined satisfies the following essential property (Yang–Baxter equation) shown on Fig. 2. The vertex with diagonal edges is assigned weights (the so-called R matrix) which are the same as the usual weights, up to a shift of the difference of the spectral parameter. Here we shall not need the explicit expression of the R matrix.

Fig. 2: Yang–Baxter equation. Summation over arrows of the *internal* edges is implied, whereas external arrows are fixed.

We shall now list the following four properties which determine entirely $Z_N(\{\lambda_i\}, \{\mu_k\})$ and sketch their proof (for a detailed algebraic proof the reader is referred to [11]):

a) $Z_1 = \sinh(2\gamma)$.

This is by definition.

b) $Z_N(\{\lambda_i\}, \{\mu_k\})$ is a symmetric function of the $\{\lambda_i\}$ and of the $\{\mu_k\}$.

It is sufficient to prove that exchange of μ_i and μ_{i+1} (for any i) leaves the partition

function unchanged. This can be obtained by repeated use of the Yang–Baxter property:

$$\begin{aligned}
R_{\downarrow\downarrow}(\mu_i - \mu_{i+1}) Z_N(\{\dots \mu_i, \mu_{i+1} \dots\}) &= \begin{array}{c} \text{Diagram showing a 4x4 grid of arrows with a crossing at } \mu_i \text{ and } \mu_{i+1} \text{ in the middle row. The crossing is a standard Yang-Baxter crossing: top-left to bottom-right, top-right to bottom-left. Arrows point generally from left to right and top to bottom. Labels } \mu_i \text{ and } \mu_{i+1} \text{ are at the bottom.} \end{array} = \\
&= \begin{array}{c} \text{Diagram showing a 4x4 grid of arrows with a crossing at } \mu_i \text{ and } \mu_{i+1} \text{ in the middle row. The crossing is a standard Yang-Baxter crossing: top-left to bottom-right, top-right to bottom-left. Arrows point generally from left to right and top to bottom. Labels } \mu_i \text{ and } \mu_{i+1} \text{ are at the bottom.} \end{array} \\
&= \dots = \begin{array}{c} \text{Diagram showing a 4x4 grid of arrows with a crossing at } \mu_i \text{ and } \mu_{i+1} \text{ in the middle row. The crossing is a standard Yang-Baxter crossing: top-left to bottom-right, top-right to bottom-left. Arrows point generally from left to right and top to bottom. Labels } \mu_i \text{ and } \mu_{i+1} \text{ are at the bottom.} \end{array} = R_{\uparrow\uparrow}(\mu_i - \mu_{i+1}) Z_N(\{\dots \mu_{i+1}, \mu_i \dots\})
\end{aligned} \tag{2.4}$$

where $R_{\uparrow\uparrow} = R_{\downarrow\downarrow}$ is the appropriate entry of the R matrix; and similarly for the $\{\lambda_i\}$.

c) $Z_N(\{\lambda_i\}, \{\mu_k\}) = e^{-(N-1)\lambda_i} P_{N-1}(e^{2\lambda_i})$ where P_{N-1} is a polynomial of degree $N-1$, and similarly for the μ_k .

Let us choose one configuration. Then the only weights which depend on λ_i are the N weights on row i . Since the outgoing arrows are in opposite directions, at least one of the weights must be c . Therefore there are at most $N-1$ weights a and b , and the product of all weights is of the form $e^{-(N-1)\lambda_i} P_{N-1}(e^{2\lambda_i})$. This property remains of course valid when we sum over all configurations.

d) $Z_N(\{\lambda_i\}, \{\mu_k\})$ obeys the following recursion relation:

$$\begin{aligned}
Z_N(\{\lambda_i\}, \{\mu_k\})_{|\lambda_j - \mu_l = \gamma} &= \sinh(2\gamma) \prod_{\substack{1 \leq k \leq N \\ k \neq l}} \sinh(\lambda_j - \mu_k + \gamma) \\
&\quad \prod_{\substack{1 \leq i \leq N \\ i \neq j}} \sinh(\lambda_i - \mu_l + \gamma) Z_{N-1}(\{\lambda_i\}_{i \neq j}, \{\mu_k\}_{k \neq l})
\end{aligned} \tag{2.5}$$

Because of property b), we can assume that $j = l = 1$. Since $\lambda_k - \mu_l = \gamma$ implies $a(\lambda_j - \mu_l) = 0$, by inspection all configurations with non-zero weights are of the form shown on Fig. 3. This immediately proves Eq. (2.5).

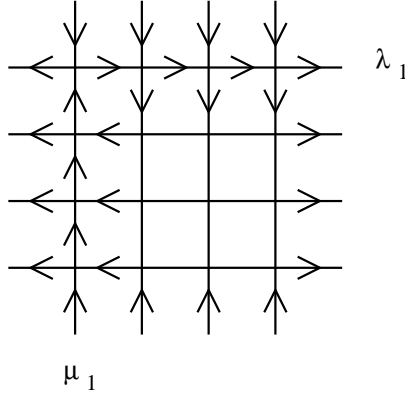


Fig. 3: Graphical proof of the recursion relation.

It is easy to see that the four properties a), b), c) and d) characterize entirely $Z_N(\{\lambda_i\}, \{\mu_k\})$. This is enough to prove that $Z_N(\{\lambda_i\}, \{\mu_k\})$ has the following determinant representation [11]:

$$Z_N(\{\lambda_i\}, \{\mu_k\}) = \frac{\prod_{1 \leq i, k \leq N} \sinh(\lambda_i - \mu_k + \gamma) \sinh(\lambda_i - \mu_k - \gamma)}{\prod_{1 \leq i < j \leq N} \sinh(\lambda_i - \lambda_j) \prod_{1 \leq k < l \leq N} \sinh(\mu_k - \mu_l)} \det_{1 \leq i, k \leq N} \left[\frac{\sinh(2\gamma)}{\sinh(\lambda_i - \mu_k + \gamma) \sinh(\lambda_i - \mu_k - \gamma)} \right] \quad (2.6)$$

Indeed, one can check that this expression satisfies the four properties listed above.

The expression (2.6) might seem singular when two spectral parameters λ_i and λ_j coincide (and similarly for the μ_k); but in fact the pole created by the factor $\sinh(\lambda_i - \lambda_j)$ is compensated by the zero of the determinant due to the fact that two rows are identical. Therefore, particular care must be taken when considering the homogeneous limit where all the λ_i are equal (and all the μ_k). This limit was studied in detail in [11], and we shall simply summarize the result of the calculation. Let us call t the common value of $\lambda_i - \mu_k$ for all i and k . When the λ_i are close to one another one must Taylor expand the function

$$\phi(t) \equiv \frac{\sinh(2\gamma)}{\sinh(t + \gamma) \sinh(t - \gamma)} \quad (2.7)$$

which appears in the determinant. This leads to the following expression:

$$Z_N(t) = \frac{(\sinh(t + \gamma) \sinh(t - \gamma))^{N^2}}{\left(\prod_{n=0}^{N-1} n! \right)^2} \det_{1 \leq i, k \leq N} \left[\frac{d^{i+k-2}}{dt^{i+k-2}} \phi(t) \right] \quad (2.8)$$

3. Determinant representation and Toda chain hierarchy

We shall now investigate the properties of the determinant which appears in Eq. (2.8), and for which we introduce the notation

$$\tau_N(t) = \det_{1 \leq i, k \leq N} [m_{i+k-2}] \quad (3.1)$$

with

$$m_n = \frac{d^n}{dt^n} \phi(t) \quad (3.2)$$

Let us write down the bilinear Hirota equation satisfied by the τ_N . For completeness, we recall that they are a consequence of Jacobi's determinant identity:

$$(3.3)$$

The large squares represent a given matrix, and the shaded regions are the sub-matrices whose determinants one must consider. Applying it to τ_{N+1} (up to a re-shuffling of the rows and columns), we find [12]:

$$\tau_N \tau_N'' - \tau_N'^2 = \tau_{N+1} \tau_{N-1} \quad \forall N \geq 1 \quad (3.4)$$

where primes denote differentiation with respect to t . This is supplemented by the initial data: $\tau_0 = 1$ and $\tau_1 = \phi$. Equivalently, we have:

$$(\log \tau_N)'' = \frac{\tau_{N+1} \tau_{N-1}}{\tau_N^2} \quad \forall N \geq 1 \quad (3.5)$$

which is the form of the equation that we shall use.

Note that if we introduce the combinations $e^{\varphi_N} = \tau_N / \tau_{N-1}$, $N \geq 1$, Eq. (3.5) implies for the φ_N :

$$\varphi_N'' = e^{\varphi_{N+1} - \varphi_N} - e^{\varphi_N - \varphi_{N-1}} \quad \forall N \geq 2 \quad (3.6)$$

and $\varphi_1'' = e^{\varphi_2 - \varphi_1}$. These are the usual Toda (semi-infinite) chain equations [16], [17], [18]. Another possible form is

$$\psi_N'' = - \sum_M C_{MN} e^{\psi_M} \quad N \geq 1 \quad (3.7)$$

with $\psi_N = \varphi_{N+1} - \varphi_N$ and C_{MN} ($M, N \geq 1$) the Cartan matrix of the semi-infinite diagram A_∞ .

This suggests a connection with the Toda chain hierarchy [19], [20], [21], [22], [23]. Indeed, let us mention that given a H  nkel matrix (m_{i+k-2}) – i.e. whose entries only depend on $i+k$ – the m_n can be made to depend on a set of parameters $\{t_q\}_{q \geq 1}$ in such a way that the determinants τ_N become τ -functions of the whole Toda (semi-infinite) chain hierarchy [20]. Namely, one must choose

$$m_n(\{t_q\}) = \int d\rho(x) x^n e^{\sum_{q \geq 1} t_q x^q} \quad (3.8)$$

where $d\rho(x)$ is an arbitrary measure¹ (in the matrix model context [20], the t_q are the coefficients of the polynomial potential). Here, we are in the simplest situation where only one parameter $t_1 \equiv t$ is allowed to evolve. We immediately check that Eq. (3.8) implies that $m_n(t) = \frac{d^n}{dt^n} m_0(t)$, which is consistent with Eq. (3.2).

4. The thermodynamic limit

We shall now consider the thermodynamic (i.e. large N) limit of the expression (2.8) in the various regimes of the six-vertex model. For that we shall use the Hirota equation in its form (3.5).

When $N \rightarrow \infty$ it is expected that the partition function behaves in the following way:

$$\log Z_N(t) = -N^2 F(t) + O(N) \quad (4.1)$$

where $F(t)$ is the *bulk free energy* (we shall always set the temperature $k_B T = 1$). Our main goal is to compute explicitly $F(t)$.

Comparing the expected asymptotic (4.1) with the exact formula (2.8), we find that the determinant τ_N must be of the form

$$\tau_N = \left(\prod_{n=0}^{N-1} n! \right)^2 e^{N^2 f(t) + O(N)} \quad (4.2)$$

where

$$f(t) = -F(t) - \log(\sinh(t + \gamma) \sinh(t - \gamma)) \quad (4.3)$$

¹ This must be considered as a formal expression; e.g. the measure may not necessarily be positive.

We now want to substitute the expansion (4.2) into the equation (3.5). For that we need to assume that the subdominant corrections to the bulk free energy vary slowly as a function of N ; we shall discuss the validity of this assumption below. We then find that the expansion is consistent since both left and right hand sides of (3.5) turn out to be of order N^2 . The resulting equation for f is:

$$f'' = e^{2f} \quad (4.4)$$

This is an ordinary second order differential equation, which can be readily solved. The general solution depends on two parameters α and t_0 :

$$e^{f(t)} = \frac{\alpha}{\sinh(\alpha(t - t_0))} \quad (4.5)$$

If the weights are chosen to be real, then the free energy should be real and this implies that α must be real or purely imaginary.

So far everything we have done was independent of the particular form of the function $\phi(t)$ and therefore independent of γ . In order to fix the two constants in (4.5), we must now discuss separately the different regimes of the six-vertex model. Let us recall that the latter are usually distinguished by the value of the parameter (cf Eq. (8.3.21) of [3])

$$\Delta = \frac{a^2 + b^2 - c^2}{2ab} \quad (4.6)$$

The weights a, b, c were defined in Eq. (2.3) (with $\lambda - \mu \equiv t$). In this parameterization,

$$\Delta = \cosh(2\gamma) \quad (4.7)$$

4.1. Ferro-electric phase: $\Delta > 1$

This corresponds to the parameters γ and t real; we recall that the weights are given by

$$a = \sinh(t - \gamma) \quad b = \sinh(t + \gamma) \quad c = \sinh(2\gamma) \quad (4.8)$$

with $|\gamma| < t$. This is the so-called ferroelectric phase. In the case of periodic boundary conditions, it is known that the system is frozen in its ground state configuration, in which all arrows are aligned: if $a > b$ all arrows point up and to the right or down and to the left, whereas if $b > a$ they point up and to the left or down and to the right. The domain wall boundary conditions do not allow all arrows to be aligned: the ground state will instead take the form of Fig. 4. However at leading order in the large N limit, this does not affect the free energy, and we expect to find the same result as for periodic boundary conditions.

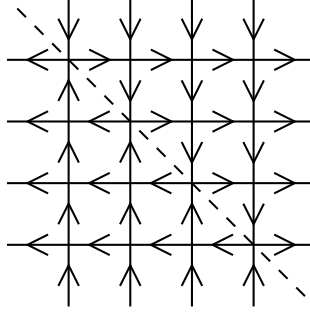


Fig. 4: Ground state configuration of the ferroelectric phase (for $b > a$; the case $a > b$ is obtained by taking the mirror image).

Indeed, it is easy to see that the relevant solution of Eq. (4.4) is

$$e^{f(t)} = \frac{1}{\sinh(t - |\gamma|)} \quad (4.9)$$

and therefore the bulk free energy takes the form

$$e^{-F(t)} = \sinh(t + |\gamma|) = \max(a, b) \quad (4.10)$$

in agreement with the case of periodic boundary conditions.

4.2. Disordered phase: $-1 < \Delta < 1$

In this regime, it is customary to make the following redefinitions:

$$\gamma' = i(\gamma + i\pi/2) \quad (4.11)$$

$$t' = i(t + i\pi/2) \quad (4.12)$$

and divide all the weights by i , so that they take the form:

$$a = \sin(\gamma - t) \quad b = \sin(\gamma + t) \quad c = \sin(2\gamma) \quad (4.13)$$

and $\Delta = -\cos(2\gamma)$. Using symmetry considerations, one can always assume $0 < \gamma < \pi/2$. We only consider the region $|t| < \gamma$ (where the weights are positive).

Taking into account these redefinitions, the partition function becomes:

$$Z_N(t) = \frac{(\sin(t + \gamma) \sin(t - \gamma))^{N^2}}{\left(\prod_{n=0}^{N-1} n!\right)^2} \det_{1 \leq i, k \leq N} \left[\frac{d^{i+k-2}}{dt^{i+k-2}} \phi(t) \right] \quad (4.14)$$

with a redefined $\phi(t) = \sin(2\gamma)/(\sin(t - \gamma) \sin(t + \gamma))$; the determinant τ_N still satisfies Eq. (3.4) and $f(t)$ defined by (4.3) is still a solution of Eq. (4.4).²

Let us mention that the partition function has been computed exactly [24] at three particular values of the parameters: $t = 0$, $\gamma = \pi/6$, $\pi/4$ and $\pi/3$. In all three cases the expansion (4.1) and the assumption of smoothness of the sub-dominant corrections (which is necessary to derive the ordinary differential equation (4.4)) can be checked exactly. We have also checked it numerically for a variety of values of t and γ .

We must now select the appropriate solution (of the form (4.5)) of the Eq. (4.4). Let us first assume that $|t| < \gamma$ (this is the only physical region, i.e. where all the weights are positive). It is easy to check that $f(t)$ must be an even function of t . The only even solution of Eq. (4.4) is

$$e^{f(t)} = \frac{\alpha}{\cos(\alpha t)} \quad (4.15)$$

where α remains to be determined. Note that this implies for $F(t)$

$$e^{-F(t)} = \sinh(\gamma - t) \sinh(\gamma + t) \frac{\alpha}{\cos(\alpha t)} \quad (4.16)$$

We must then use the boundary condition given by $|t| = \pm\gamma$. At these values one can compute directly $Z_N(t)$. Indeed the only non-zero configurations are of the form of Fig. 4, and we find

$$Z_N(t = \pm\gamma) = \sin(2\gamma)^{N^2} \quad (4.17)$$

and therefore $e^{-F(t)} = \sin(2\gamma)$. Since the prefactor in (4.16) vanishes when $|t| = \gamma$, we conclude that α must be chosen in such a way that $\cos(\alpha t)$ is non-zero for $|t| < \gamma$, but vanishes as $|t| = \gamma$. This uniquely determines α to be: $\alpha = \frac{\pi}{2\gamma}$. We obtain the final expression

$$e^{-F(t)} = \sin(\gamma - t) \sin(\gamma + t) \frac{\pi/2\gamma}{\cos(\pi t/2\gamma)} \quad (4.18)$$

As a consistency check, one takes the limit $t \rightarrow \pm\gamma$ and finds $e^{-F(t)} = \sin(2\gamma)$, as it should be.

For further checks, let us set $t = 0$; a more standard normalization of the weights is then

$$a = b = 1 \quad c = 2 \cos \gamma \quad (4.19)$$

² Note that the sign is unchanged in Eq. (4.4); this is the combined effect of the “Wick rotation” of t ($t \rightarrow it$) and of dividing all the weights by i ($e^f \rightarrow -i e^f$).

and the bulk free energy becomes

$$e^{-F} = \frac{\pi}{2} \frac{\sin \gamma}{\gamma} \quad (4.20)$$

At $\gamma = \pi/6, \pi/4, \pi/3$, the values predicted by (4.20) coincide with the large N limit of the expressions of [24]. Also, this fits perfectly with some numerical computations of the determinant we have performed.

We can compute the bulk energy (energy per unit site), which turns out to be

$$E = (\cot \gamma - 1/\gamma) \cot \gamma \log(2 \cos \gamma) \quad (4.21)$$

Fig. 5 shows the comparison with Montecarlo simulations. The agreement is also very good.

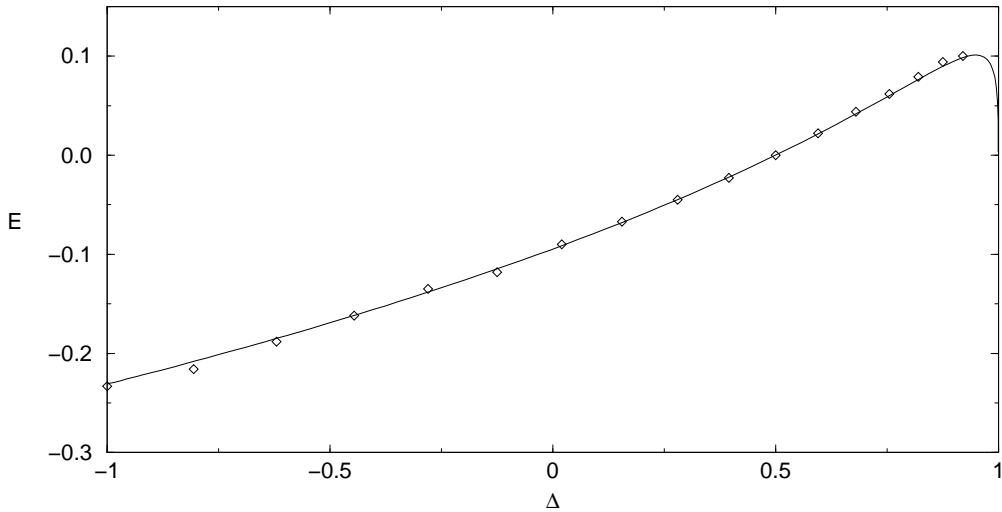


Fig. 5: Energy E as a function of the anisotropy Δ . The curve is given by Eq. (4.21), whereas the diamonds are the results of Montecarlo simulations on lattices of size $N = 64$.

Finally let us mention that there seems to be no simple relation between the PBC and DWBC bulk free energies: from an analytic point of view, the DWBC free energy is an elementary function, whereas the PBC free energy is given by a non-trivial integral. Furthermore, the DWBC free energy is always greater than the PBC free energy, even at infinite temperature ($\Delta = 1/2$), see Fig. 6.

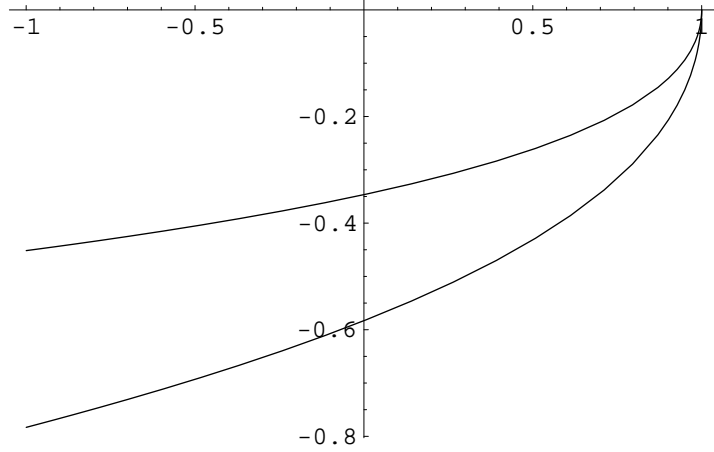


Fig. 6: Bulk free energies for PBC and DWBC as a function of Δ .

4.3. Anti-ferroelectric phase: $\Delta < -1$

In this phase, the smoothness assumption of the sub-dominant corrections to the bulk free energy is *not* satisfied, as can be clearly seen numerically. The ratio $Z_{N+1}Z_{N-1}/Z_N^2$ does not converge in the large N limit but instead has a pseudo-periodic behavior reminiscent of the one-matrix model with several cuts [25], and slightly more sophisticated methods are needed to analyze the large N limit. We leave this to a future publication.

4.4. Phase transition at $\Delta = 1$

If the Boltzmann weights depend on a parameter (e.g. temperature), it is known that with periodic boundary conditions, the system undergoes phase transitions as Δ crosses ± 1 . Let us use the expressions of the bulk free energy found above to clarify what happens in the case of domain wall boundary conditions.

Here we shall consider the transition from ferroelectric (low temperature) to disordered (high temperature) regime, that is from $\Delta > 1$ to $\Delta < 1$. The parameter that plays the role of deviation from criticality $T - T_c$ can be defined as

$$T - T_c \equiv 1 - \Delta \quad (4.22)$$

We assume that $b > a$ (the case $a > b$ can be treated similarly), and re-scale the weights so that $b = 1$. With this convention, we simply have in the ferroelectric phase:

$$e^{-F} = 1 \quad \Delta > 1 \quad (4.23)$$

(cf Eq. (4.10)). Let us now consider $\Delta \rightarrow 1^-$. The weights are

$$a = \frac{\sin(\gamma - t)}{\sin(\gamma + t)} \quad b = 1 \quad c = \frac{\sin(2\gamma)}{\sin(\gamma + t)} \quad (4.24)$$

with $\gamma = \pi/2 + \epsilon$, $t = \pi/2 + \epsilon x$; x must be kept fixed as $\epsilon \rightarrow 0$. Note that $\Delta = \cos(2\epsilon)$, so that

$$T - T_c \propto \epsilon^2 \quad (4.25)$$

Expanding the expression (4.18) for the free energy, we obtain:

$$e^{-F} = 1 - \frac{2(x-1)^2}{3\pi} \epsilon^3 + O(\epsilon^4) \quad (4.26)$$

Comparing (4.23) and (4.26), we find a *second order* phase transition, with a singular part $(T - T_c)^{3/2}$ corresponding to a critical exponent $\alpha = -1/2$. This is to be contrasted with the first order phase transition that occurs in the case of PBC. Let us however emphasize that the difference of orders of the phase transitions is not that significant, since the phase transition is somewhat special (in the case of PBC, the correlation length jumps from zero for $\Delta > 1$ to infinity for $\Delta < 1$).

5. Comments and conclusion

In this work, we have computed explicitly the large N asymptotic behavior of a $N \times N$ determinant which plays the role of partition function of the six-vertex model with domain wall boundary conditions. This gives rise to particularly simple expressions for the bulk free energy of this model (Eqs. (4.10) and (4.18)). Let us immediately mention another interpretation of this quantity. Six-vertex model arrow configurations with domain wall boundary conditions on a $N \times N$ lattice are in one-to-one correspondence with *alternating sign matrices* (ASM) of size N , that is square matrices with entries 0 or ± 1 such that each row and column has an alternating sequence of $+1$ and -1 (zeroes excluded) starting and ending with a $+1$. The correspondence assigns a 0 to each vertex of type a or b and $+1$ (resp. -1) to the first (resp. second) vertex of type c , cf Eq. (2.2). Therefore, the number of ASM is exactly equal to the partition function considered before with $a = b = c = 1$. For our purposes let us define a refined counting (x -enumeration in the language of [24]) by assigning a weight x to each entry -1 of the ASM. The resulting quantity $A(N, x)$ is still related to the six-vertex model; indeed, one can easily show that

$$A(N, x) = x^{-N/2} Z_N(a = b = 1, c = \sqrt{x}) \quad (5.1)$$

If $0 \leq x \leq 4$, one can set $x = 4 \cos^2 \gamma$ and the weights are of the form (4.19). One can then prove (extending slightly the asymptotic expansion found in 4.2) that

$$\log A(N, x) = N^2 \log \left[\frac{\pi \sin \gamma}{2 \gamma} \right] - \frac{N}{2} \log x + O(\log N) \quad \forall x \in [0, 4] \quad (5.2)$$

Finally, let us mention that an important question is to physically interpret the discrepancy of the bulk free energy found when comparing domain wall and periodic boundary conditions of the six-vertex model, which is somewhat contrary to standard lore on the thermodynamic limit of statistical models. One clue is to notice another equivalence, this time of domino tilings (i.e. dimers on a square lattice in a dual description) and six-vertex model at $\Delta = 0$ – both models are well-known to describe essentially one Dirac fermion. The more precise statement is that the counting of domino tilings of the *Aztec diamond* (see [7]) is exactly equivalent to the six-vertex model with domain wall boundary conditions at $a = b = 1, c = \sqrt{2}$. These tilings have been an object of interest for mathematicians, see in particular [8], [13]. The “arctic circle theorem” [7] shows that as the size of the system grows large, the domino configurations become frozen outside the circle inscribed inside the diamond, and remain disordered but still heterogeneous [8] (i.e. non translationally invariant) inside the circle. These statements have a straightforward equivalent in the six-vertex language, and do give a qualitative understanding of the dependence of the bulk free energy on the boundary conditions at the particular value $\Delta = 0$. It would be most interesting to find a “generalized arctic circle theorem” for any value of the parameter Δ of the six-vertex model.

Acknowledgements

It is a pleasure to acknowledge stimulating discussions with F.Y. Wu, S. Ruijsenaars, B. Mc Coy, R. Shrock, M. Wadati; and with R. Behrends (who participated in the early stages of this project).

References

- [1] E. Lieb, *Phys. Rev.* 18 (1967), 1046; 19 (1967), 108.
- [2] B. Sutherland, *PRL* 19 (1967), 103.
- [3] R.J. Baxter, *Exactly Solved Models in Statistical Mechanics* (San Diego, CA: Academic).
- [4] P.W. Kasteleyn, *Physica* 27 (1960), 1209.
- [5] M.E. Fisher, *Phys. Rev.* 124 (1961), 1664.
- [6] W.T. Lu and F.Y. Wu, *Phys. lett. A* 259 (1999), 108.
- [7] W. Jockush, J. Propp and P. Shor, preprint [math.CO/9801068](#).
- [8] H. Cohn, N. Elkies and J. Propp, *Duke Math. Journal* 85 (1996), 117.
- [9] V.E. Korepin, *Commun. Math. Phys* 86 (1982), 391.
- [10] A.G. Izergin, *Sov. Phys. Dokl.* 32 (1987), 878.
- [11] A.G. Izergin, D.A. Coker and V.E. Korepin, *J. Phys. A* 25 (1992), 4315.
- [12] K. Sogo, *Journal of the Physical Society of Japan* 62, 6 (1993), 1887.
- [13] N. Elkies, G. Kuperberg, M. Larsen and J. Propp, *Journal of Algebraic Combinatorics* 1 (1992), 111; 219.
- [14] D.M. Bressoud, *Proofs and Confirmations: The Story of the Alternating Sign Matrix Conjecture*, Cambridge University Press, Cambridge, 1999
- [15] D. Bressoud and J. Propp, *Notices of the AMS* June/July (1999), 637.
- [16] M. Toda *Journ. Phys. Soc. Japan* 22 (1967), 431; *Prog. Theor. Phys. Suppl.* 45 (1970), 174.
- [17] R. Hirota *Journ Phys. Soc. Japan* 56 (1987), 4285.
- [18] H. Flaschka *Phys. Rev. B* 9 (1974); *Prog. Theor. Phys.* 51 (1974), 703.
- [19] K. Ueno, K. Takasaki *Adv. Studies in Pure Math.* 4 (1984), 1.
- [20] M. Adler and P. van Moerbeke, *Duke Math. Journal* 80 (1995), 863 (preprint [solv-int/9706010](#)); preprint [math.CO/9912143](#).
- [21] O. Lipan, P.B. Wiegmann, A. Zabrodin, preprint [solv-int/9704015](#).
- [22] P.B. Wiegmann, A. Zabrodin, preprint [hep-th/9909147](#).
- [23] I. Krichever, O. Lipan, P. Wiegmann, A. Zabrodin, preprint [hep-th/9604080](#).
- [24] G. Kuperberg, *Internat. Math. Res. Notices* 3 (1996), 139 (preprint [math.CO/9712207](#)).
- [25] P. Deift, T. Kriecherbauer, K.T-R. McLaughlin, S. Venakides and X. Zhou, *Commun. on Pure and Applied Math.* 52 (1999), 1491.